

# Structure function measurements of the intermittent MHD turbulent cascade

T. S. Horbury and A. Balogh

The Blackett Laboratory, Imperial College, London, U.K.

Received: 8 September 1997 – Revised 10 February 1998 – Accepted: 27 April 1998

**Abstract.** The intermittent nature of turbulence within solar wind plasma has been demonstrated by several studies of spacecraft data. Using magnetic field data taken in high speed flows at high heliographic latitudes by the Ulysses probe, the character of fluctuations within the inertial range is discussed. Structure functions are used extensively. A simple consideration of errors associated with calculations of high moment structure functions is shown to be useful as a practical estimate of the reliability of such calculations. For data sets of around 300 000 points, structure functions of moments above 5 are rarely reliable on the basis of this test, highlighting the importance of considering uncertainties in such calculations. When unreliable results are excluded, it is shown that inertial range polar fluctuations are well described by a multifractal model of turbulent energy transfer. Detailed consideration of the scaling of high order structure functions suggests energy transfer consistent with a “Kolmogorov” cascade.

development of an inertial range is provided by the change in shape of the power spectrum of fluctuations as they travel from the Sun, especially in high speed streams (e.g., Bavassano *et al.*, 1982; Feynman *et al.*, 1996) – the spectral index at small scales is often near 5/3, the value predicted by the Kolmogorov (1941a) theory. The reader is referred to Mangeney *et al.* (1991), Roberts and Goldstein (1991) and Tu and Marsch (1995) for recent reviews of the state of turbulence studies in the heliosphere.

In this paper, we concentrate on the inertial range of turbulent fluctuations in the solar wind and in particular their “intermittent” nature. Intermittency – spatial inhomogeneity of energy transfer – is an accepted property of terrestrial fluid turbulence (see, for example, Borgas, 1992 and Frisch, 1995). Recently, several studies have demonstrated that heliospheric magnetic field and velocity fluctuations are indicative of intermittent turbulence, by considering the distributions of fluctuations (Feynman and Ruzmaikin, 1994; Marsch and Tu, 1994; Ruzmaikin *et al.*, 1995) and structure functions (Burlaga, 1991; Marsch and Liu, 1993; Ruzmaikin *et al.*, 1995; Horbury *et al.*, 1996a) – Marsch and Tu (1997) is a recent comprehensive review of this subject. Different studies have concluded that the fluctuations are in agreement with different models of intermittency in turbulence. Indeed, it is not even clear whether a description based around the Kolmogorov (1941a) hydrodynamic turbulence model or the Kraichnan (1965) and Iroshnikov (1964) MHD turbulence model is more appropriate for turbulent fluctuations in the heliosphere. The aim of this paper is to use a careful structure function analysis to study the inertial range – where comparison of models with observations is easiest – in considerable detail, to decide which models of intermittency are in agreement with data and to attempt to differentiate between Kolmogorov and Kraichnan-Iroshnikov scaling on the basis of the experimental data.

We have used magnetic field data taken by the Ulysses spacecraft within flows from the Sun’s Northern and Southern polar coronal holes to study inertial range fluctua-

## 1 Introduction

The identification of at least some fluctuations in the solar wind as turbulent is widely accepted. Coleman (1968) showed that fluctuations in the magnetic field and velocity near the Earth’s orbit had power spectra  $E(f) \propto f^{-\alpha}$ , where the spectral index  $\alpha \sim 1.2$ , on spacecraft scales of hours to minutes. Coleman interpreted these fluctuations as being inertial range turbulence, probably indicative of Kraichnan (1965) magnetohydrodynamic (MHD) turbulence. While Belcher and Davis (1971) pointed out that fluctuations in high speed streams were highly Alfvénic with an outward sense of propagation – and indeed while near-ecliptic fluctuations are often Alfvénic (e.g. Roberts *et al.*, 1987) – nevertheless they appear to be indicative of evolving turbulence. Strong evidence of this evolution and the

tions. The inertial range is not particularly large in polar flows at the distances sampled by Ulysses (Horbury *et al.*, 1995a, 1996a, b), extending up to around 100s in the spacecraft frame. However, inertial range fluctuations in undisturbed high speed polar flows exist in a much more homogeneous environment than those near the ecliptic (Phillips *et al.*, 1995; Balogh *et al.*, 1995). As such, we may expect that energy input into the inertial range, by whatever means, would be less variable than that near the ecliptic, leading to a better defined inertial range.

In sections 2 and 3, we discuss the concept of inertial range turbulence and intermittency, in both non-magnetised and MHD fluids. Several intermittency models are discussed, with emphasis placed on the physical differences between them. Section 4 gives a description of the calculation of structure functions, with emphasis on the influence of uncertainties in distributions of fluctuations on structure function results. We demonstrate that such uncertainties are significant, and can cause misleading results. In sections 5 and 6 by taking into account these restrictions on the structure function results we show that, of the models considered, the multifractal  $p$  model (Meneveau and Sreenivasan, 1987a, b) best describes the fluctuations. Finally, section 7 discusses details of the energy transfer in the turbulent cascade.

## 2 Inertial range turbulence

An essential property of the concept of inertial range turbulence is that of energy transfer between scales. In most cases, energy is transferred from large to small scales, where it is eventually dissipated as heat. Two scales can therefore be defined: that at which energy is inserted into the fluctuations,  $L_0$ , and the dissipation scale,  $l_d$ . If one assumes that the energy input rate per unit mass at scale  $L_0$ ,  $\Pi_0$ , is constant over time and space, then the energy dissipation rate  $\varepsilon = \Pi_0$ . Similarly, if the rate of energy transferred to a particular scale  $l$ ,  $L_0 > l > l_d$ , is  $\Pi(l)$ , then energy must be lost from that scale at the same rate. If  $L_0 > l > l_d$  and therefore energy is transferred through many scales before being dissipated, then we expect that the energy transfer rate per unit volume,  $\Pi$ , is independent of scale. That is,

$$\Pi(l) = \Pi_0 = \varepsilon \quad (1)$$

for  $L_0 > l > l_d$ . If the Reynolds' number is high (i.e. inertial forces dominate viscous forces) then there is essentially no dissipation in this range of scales: it is termed the inertial range. Studies of turbulence concentrate on the nature of the energy transfer process, which is not well understood.

### 2.1 Kolmogorov Turbulence

Kolmogorov (1941a), hereafter referred to as K41, introduced a model of inertial range turbulence based on the Richardson (1922) picture of a turbulent fluid containing a hierarchy of vortices on all scales (see, for example, Frisch,

1995 and also Batchelor, 1953; Monin and Yaglom, 1975; Frisch *et al.*, 1978; Paladin and Vulpiani, 1987; Matthaeus and Zhou, 1989; Zhou and Matthaeus, 1990; Mangeney *et al.*, 1991). We define characteristic velocity fluctuations on a scale  $l$  as  $u(l)$  and assume that the energy transfer rate is homogeneous and isotropic. If the energy on a particular scale is  $E(l)$  and the characteristic time for a fluctuation of size  $l$  to transfer a sizeable fraction of its energy to smaller scales is  $\tau_T$ , the energy transfer time, then

$$\varepsilon = \Pi(l) \propto E(l)/\tau_T(l). \quad (2)$$

If this energy transfer occurs by simple eddy decay, then  $\tau_T$  is proportional to the eddy turnover time,  $\tau_E$

$$\tau_T(l) \propto \tau_E(l) \propto l/u(l) \quad (3)$$

and since  $E(l) \propto u^2(l)$ , we have  $E(l) \propto (\varepsilon l)^{2/3}$  and

$$u(l) \propto (\varepsilon l)^{1/3}. \quad (4)$$

As a consequence, the moments (powers) of these velocity fluctuations scale as

$$u^m(l) \propto l^{m/3} \quad (5)$$

within the inertial range. That is, if the  $m$ -th moment of the velocity fluctuations varies with scale with exponent  $h(m)$

$$u^m(l) \propto l^{h(m)} \quad (6)$$

then for the K41 model,

$$h(m) = m/3. \quad (7)$$

The resulting power spectral index can be calculated from the scaling properties of  $u^2(l)$  (Batchelor, 1953; Monin and Yaglom, 1975). The power spectrum,  $E(f) \propto f^{-\alpha}$  where

$$\alpha = 1 + g(2) \quad (8)$$

and  $g(2) = h(2)$ . Equation (8) is a general result if the spatial averages of the velocity fluctuations,  $\langle u^m(l) \rangle$ , vary with scale with exponent  $g(m)$ , so that  $\langle u^2(l) \rangle \propto l^{g(2)}$ ; for K41,  $\langle u^2(l) \rangle = u^2(l)$  – because the fluctuations fill the entire space on every scale – and therefore  $g(m) = h(m)$ : this is not necessarily the case for intermittent turbulence, as we will see in section 3. For the K41 model, since  $g(2) = h(2) = 2/3$ ,  $\alpha = 5/3$ . The relation  $\alpha = 5/3$  is often observed in terrestrial fluid turbulence. However, measurements of the scaling properties of moments of the velocity fluctuations using structure functions (e.g. Anselmet *et al.*, 1984) show that the equality  $g(m) = m/3$  is not satisfied in general. For moments above 3, the measured values of  $g(m)$  are lower than  $m/3$ . This result is usually explained by considering the spatial intermittency of the energy transfer process, a topic to which we return in the next section.

### 2.2 Kraichnan-Iroshnikov Turbulence

Kraichnan (1965) and Iroshnikov (1964), hereafter K-I65, discussed turbulence in a plasma, and argued that the energy transfer rate should be slower than in an unmagnetised fluid. In a normal fluid or a magnetofluid, the presence

of a large scale background velocity (as a result of a flow, or due to large-scale eddies) does not affect small scale fluctuations, because it does not disrupt their interactions: it can be locally removed with a frame transformation. The addition of a background magnetic field to an incompressible magnetofluid, however, causes fluctuations in the magnetic field or velocity to propagate parallel or anti-parallel to the background field as Alfvén waves. As a result, the fluctuations tend to decorrelate in the “Alfvén decorrelation time”  $\tau_A(l)=l/V_A$ , where  $V_A$  is the Alfvén speed. If  $\tau_A(l) \ll \tau_E(l)$  then eddies cannot decay fully before they decorrelate, a process which does not transfer energy between scales. If a full eddy decay takes a time  $\tau_E$  then as a result of decorrelation only the fraction  $\tau_A/\tau_E$  of the decay will occur. Therefore, the full energy transfer takes a factor  $\tau_E/\tau_A$  longer than in the K41 case and the energy transfer time is

$$\tau_T(l) \propto \tau_E(l) \frac{\tau_E(l)}{\tau_A(l)} \quad (9)$$

$$\propto V_A \frac{l}{u^2} \propto V_A \frac{l}{b^2}$$

where  $b(l)$  is the characteristic magnetic field fluctuation due to an eddy of scale  $l$ . By the same argument as the previous section, we can then derive the spectral index and  $g(m)$  functions. The important difference between K41 and K-I65 turbulence is that decorrelation inhibits energy transfer, resulting in a slower energy transfer rate. This slower transfer rate leads to a flatter power spectrum – the spectral index  $\alpha=3/2$  in this case. Indeed, the scaling of the velocity fluctuations with scale is also shallower:

$$g(m)=m/4 \quad (10)$$

for the K-I65 model. K-I65 assumes equal amplitude Alfvénic fluctuations propagating parallel and anti-parallel to the mean field direction. This is certainly not the case in high speed polar solar wind streams, where fluctuations are largely Alfvénic with an anti-sunward sense of propagation (Goldstein *et al.*, 1995). As a result, the K-I65 model is of limited applicability to solar wind turbulence. However, the continued application of K-I65 to solar wind observations by other authors – and the lack of other MHD turbulence models – makes a detailed K41-K-I65 comparison worthwhile. More detailed discussions about the relationship between K41 and K-I65 phenomenologies can be found in, e.g. Matthaeus and Zhou (1989) and Dobrowolny *et al.* (1980). In particular, we note that if the condition  $\tau_A(l) \ll \tau_E(l)$  is not satisfied, one can have scaling between the K41 and K-I65 cases (Matthaeus and Zhou, 1989). These two cases represent limits of a continuous range of possibilities.

### 3 Intermittency of the energy transfer process

As we have noted, terrestrial measurements (e.g. Anselmet *et al.*, 1984) and *in situ* heliospheric measurements (Bur-

laga, 1991; Marsch and Liu, 1993; Horbury *et al.*, 1996a) of the scaling properties of velocity and magnetic field fluctuations, and hence of the  $g(m)$  functions, do not show the linear dependence of  $g(m)$  that is expected of the K41 or K-I65 models. This discrepancy is attributed to the spatially inhomogeneous nature of the energy transfer process – that is, it is intermittent. Several classes of model have been developed in an attempt to describe this inhomogeneity by considering details of the energy transfer process. In this section, we introduce four classes of models which have been discussed in the heliospheric turbulence literature and discuss their application to solar wind fluctuations.

#### 3.1 The $\beta$ model

Frisch *et al.* (1978) discussed a model of inertial range turbulence which attempted to describe the intermittent nature of the turbulent cascade. This model, as is the case for all the fluid models we will describe here, is an extension of the K41 formalism.

In K41 turbulence, an eddy decays and produces a number of daughters that fill the space occupied by the parent. In the  $\beta$  model, not all the space is filled (not all possible daughter eddies are produced), leaving gaps in the fluctuations on every scale.

We define the parameter  $\mu$  as a measure of the intermittency of the fluctuations:  $\mu=0$  corresponds to the K41 case. This is related to  $\beta$ , the fraction of daughter eddies produced,  $\beta=2^{-\mu}$ .

Because fluctuations occupy progressively less space on smaller scales than in the K41 case, velocity fluctuations in active eddies decrease less rapidly with decreasing scale in the  $\beta$  model. The scaling of moments of velocity fluctuations in active eddies is

$$h(m)=(1-\mu)(m/3). \quad (11)$$

Values of  $u(l)$  calculated for the K41 case corresponded to both velocity fluctuations over eddies of scale  $l$  and average velocity perturbations on a scale  $l$  because all space is filled by eddies of all scales within the inertial range. This is not the case in the  $\beta$  model, and we must therefore distinguish these two values. We define the functions,

$$S(m,l)=\left\langle \left| u_i(x+l)-u_i(x) \right|^m \right\rangle \quad (12)$$

which are called structure functions, where  $i$  denotes a component of the velocity and  $\langle \cdot \rangle$  represents an average over the data set of values of  $u(x)$ .  $S(m,l)$  is the  $m^{\text{th}}$  moment of the distribution of fluctuations in the  $i^{\text{th}}$  component of  $u$  on the scale  $l$  sampled over the fluid. We note that structure functions can be defined in other ways (for example, using vector differences, or not taking the modulus of differences: see Monin and Yaglom, 1975). Structure functions can be calculated from experimental data in a straightforward way. Details and subtleties of the method are described later in this paper.

If fluctuations are entirely space-filling at every scale, then values of  $S(m,l)$  should scale like those of  $u^m(l)$ , which are the amplitudes of fluctuations in active eddies only. As a result, if  $u^m(l)$  scales like Eq.(6), then

$$S(m,l) \propto l^{\beta(m)} \quad (13)$$

where  $g(m)=h(m)$ . However, this is not the case for the  $\beta$  model. In this case, values of  $g(m)$  are given by

$$g(m)=m/3+\mu(1-m/3). \quad (14)$$

We note that the  $\beta$  model reduces to K41 when  $\mu=0$ , as expected, and that  $g(3)=1$  for the  $\beta$  model, as is the case for K41. Indeed, the result  $g(3)=1$  follows from the Navier-Stokes equations at high Reynolds numbers (Kolmogorov, 1941b; Vainshtein and Sreenivasan, 1994) and is observed experimentally in terrestrial plasmas (Anselmet *et al.*, 1984).

Equation (14) shows that values of  $g(m)$  for the  $\beta$  model in the presence of intermittency are lower than those for K41 for  $m>3$  and higher for  $m<3$ . The spectral index  $\alpha$  is related to the scaling of  $S(m=2,l)$  – and hence  $g(2)$  – by Eq.(8), and is given by

$$\alpha=5/3+\mu/3. \quad (15)$$

Therefore, the power spectrum is steeper than in the non-intermittent case. A simple comparison of the power spectral index with the K41 value is therefore not sufficient to identify inertial range turbulence: the presence of intermittency can alter the observed spectral index despite the presence of a K41 cascade.

The  $\beta$  model predicts a linear dependence of  $g$  on  $m$ . Experimentally, observations of  $g(m)$  tend to show a non-linear dependence (see, for example, Borgas, 1992 for a discussion of various intermittency models). Consequently, other intermittency models have been proposed.

Recently, Ruzmaikin *et al.* (1995) extended the  $\beta$  model to MHD turbulence – that is, they added intermittency to the K-I65 model in the same way that Frisch *et al.* (1978) added intermittency to K41. The derivation is similar to the K41  $\beta$  model, but with the K-I65 transfer time given by Eq.(9) used instead of that for K41 fluid turbulence (Eq.3). The structure function scaling exponents in this case are given by

$$g(m)=m/4+\mu(1-m/4) \quad (16)$$

and consequently the spectral index  $\alpha=3/2+\mu/4$ . As in the non-MHD case, intermittency increases the spectral index. Ruzmaikin *et al.* (1995) and Horbury *et al.* (1996a) suggested that observations of  $g(m)$  for polar fluctuations were consistent with the Ruzmaikin *et al.* (1995) MHD  $\beta$  model, with  $\mu\sim 0.6$ .

### 3.2 The Random $\beta$ Model

Paladin and Vulpiani (1987) extended the  $\beta$  model to include the possibility that turbulent fluctuations (“eddies”) decayed into eddies with a variety of different “shapes”

with different dimensions. We do not present a derivation of the so-called random  $\beta$  model here, but simply quote the resulting values of  $g(m)$ . Paladin and Vulpiani (1987) found good agreement with the experimental data of Anselmet *et al.* (1984) by choosing space-filling eddies (corresponding to  $\beta=1$  in the  $\beta$  model) and sheets ( $\beta=1/2$ ) with different occurrence probabilities, leading to a probability distribution of  $\beta$ ,

$$P(\beta) = x\delta(\beta-1/2)+(1-x)\delta(\beta-1) \quad (17)$$

with  $x=0.125$  – that is, eddies were generated much more often than 2D sheet-like structures. By using this probability distribution of  $\beta$  rather than a single value, Paladin and Vulpiani (1987) derived the values of  $g(m)$ :

$$g(m) = m/3 - \log_2\{\beta^{(1-m/3)}\} \quad (18)$$

where  $\{\cdot\}$  denotes an average over the  $P(\beta)$  distribution. The random  $\beta$  model reduces to the  $\beta$  model if  $P(\beta)=\delta(\beta-1)$  and the K41 model if  $P(\beta)=1$ .

Burlaga (1991) showed that the random  $\beta$  model was consistent with the structure function scaling of turbulent velocity fluctuations on spacecraft scales of 0.85 to 13.6 hours at 8.5 AU using a 5 day interval of 96s samples, containing around 4500 data points.

One can apply the random  $\beta$  model to Kraichnan turbulence, as with the  $\beta$  model, by replacing the K41 energy transfer time of Eq.(3) with the K-I65 value given by Eq.(9). In this case, one obtains  $g(m)$  values given by

$$g(m) = m/4 - \log_2\{\beta^{(1-m/4)}\}. \quad (19)$$

### 3.3 The p model

Meneveau and Sreenivasan (1987a, b) developed a different method of introducing intermittency via eddy breakdown. While the  $\beta$  and random  $\beta$  models describe the effects of energy being distributed equally to only a subset of daughter eddies, the p model of Meneveau and Sreenivasan considers the effects of unequal energy distribution to daughter eddies: all eddies have some energy, but some have more than others. If we imagine that an eddy decays into two daughters, then one receives a fraction  $p$  of the parent’s energy and the other  $1-p$ . Conventionally, we take  $p\geq 1/2$ .

Recently, Tu *et al.* (1996) presented a clear derivation and discussion of the p model. Values of  $g(m)$  for the p model are given by

$$g(m) = 1 - \log_2\left(p^{m/3} + (1-p)^{m/3}\right) \quad (20)$$

As expected, the p model reduces to K41 if  $p=1/2$ :  $p=1$  is the most intermittent case. As with the  $\beta$  and random  $\beta$  models, the p model has  $g(3)=1$  independent of intermittency. We note that the p model is multifractal: the energy dissipation is distributed throughout space as a multifractal (see, for example, Frisch, 1995). It appears that energy dissipation in turbulent fluids is indeed multifractal, and the

p model has proved to be a good description of the observed structure function scaling in neutral fluid turbulence (Frisch, 1995; Borgas, 1992).

Carbone (1994) showed that the p model was in agreement with the values of  $g(m)$  observed by Burlaga (1991), with  $p=0.7$ . Carbone (1993) applied the p model to Kraichnan (1965) turbulence to produce the MHD p model, which has structure function scaling exponents given by

$$g(m) = 1 - \log_2 \left( p^{m/4} + (1-p)^{m/4} \right) \quad (21)$$

### 3.4 The She and Leveque model

She and Leveque (1994) introduced a model of intermittency which emphasises the structure of the smallest scale, dissipative, structures in the turbulent fluid. She and Leveque assumed that these structures are filaments (that is, they are essentially one dimensional) in neutral fluid turbulence. Using a K41 energy transfer scaling, they derived structure function scaling exponents given by

$$g(m) = m/9 + 2 \left( 1 - (2/3)^{m/3} \right) \quad (22)$$

This model is of particular interest because it contains no freely adjustable parameters: the dimension of the dissipation structures and the energy scaling are the only inputs, although She and Leveque also assumed a universal scaling relation between moments of spatial fluctuations in the turbulent energy transfer. Equation (22) is in good agreement with experimental observations of fully developed neutral fluid turbulence.

Grauer *et al.* (1994) extended the She and Leveque (1994) model to the MHD case. Taking a K-I65 energy transfer scaling, and assuming that the dissipative structures are sheets (for example, current sheets) they derived the following relation

$$g(m) = m/8 + 1 - (1/2)^{m/4} \quad (23)$$

Grauer *et al.* showed that the ratios  $g(m)/g(4)$  (hence artificially imposing the K-I65 condition of  $g(4)=1$ ) agreed with those measured by Burlaga (1991).

It is possible to alter the She and Leveque (1994) model to use a K41 energy transfer time, but with sheet (two dimensional) dissipative structures rather than filaments: we are grateful to one of the referees for pointing out this possibility. It is simple to show that in this case, the scaling functions of moments of the energy dissipation are, using similar terminology to She and Leveque,

$$\tau_m = \frac{2m}{3} + 1 - (1/3)^m \quad (24)$$

where  $\tau_m$  is the scaling exponent of the  $m^{\text{th}}$  moment of the energy dissipation (this is equivalent to Eq.(9) of She and Leveque, 1994). These functions are related to structure function scaling exponents as  $g(m) = m/3 + \tau_{m/3}$  and therefore

$$g(m) = m/9 + 1 - (1/3)^{m/3} \quad (25)$$

for K41 energy transfer where dissipation is confined to two dimensional sheets. We will return to this result in section 6.

## 4 Structure function calculations

In this paper, we use structure functions to analyse inertial range turbulence in the polar heliosphere. Fluctuations in high latitude solar wind flows are particularly appropriate for turbulence studies for several reasons. Firstly, the lack of stream structure at high latitudes (Balogh *et al.*, 1995; Phillips *et al.*, 1995) means that long intervals of nearly-stationary data are available, which is not the case at low latitudes. Secondly, this lack of stream structure allows turbulent evolution to proceed undisturbed, at a rather slow rate (Horbury *et al.*, 1996b). Energy appears to be inserted into the turbulent cascade from the decay of low frequency Alfvén waves: this slow process means that energy transfer through the cascade is likely to occur at a rather more constant rate than at low latitudes, where the fluctuations can be “driven” by shocks, compressions and so on. The lack of variation in the rate of polar energy transfer means that, although the inertial range is small, covering between one and two orders of magnitude in scale, it is, as we will show in this section, actually rather well defined. For an inertial range to be present, we require that energy input into the range is constant over several energy transfer times: this is plausibly the case for small scale fluctuations in the polar heliosphere where the energy input rate is likely to vary over very long timescales compared to the small scale energy transfer time. Therefore, we expect polar fluctuations to contain an inertial range which, though small because the turbulence is not fully-developed, is nevertheless well defined - the energy transfer rate is in quasi-equilibrium on these small scales. This has indeed proved to be the case.

Before presenting our results, we discuss the calculation of structure functions in some detail, with particular emphasis on their limitations. As we have seen, structure functions provide a simple method of deriving important information about the scaling and intermittency of turbulent flows and can be used to differentiate between different models of these processes in a way that is not possible using power spectra. In this work, we calculate structure functions as

$$S(m, \tau) = \left\langle \left| b_i(t+\tau) - b_i(t) \right|^m \right\rangle \quad (26)$$

where  $b_i(t)$  denotes a measurement of the  $i^{\text{th}}$  component of the magnetic field at time  $t$ . This is very similar to Eq.(12) – however, rather than taking spatial samples, time series of the magnetic field in the high speed solar wind flowing past the spacecraft are used. The high flow speed, around 750 km/s (Phillips *et al.*, 1995), means that temporal samples are essentially radial spatial samples of fluctuations (see, for example, Horbury *et al.*, 1996b).

We note in passing that it is not possible to use Ulysses bulk plasma data on the small scales considered here due to its limited time resolution (around 240s at best). However, the highly Alfvénic and incompressible nature of polar fluctuations (Goldstein *et al.*, 1995) means that magnetic field fluctuations are very similar to bulk plasma fluctuations on these scales. Of course, the field and plasma fluctuations are not identical (they are not purely Alfvénic: no energy transfer would occur in this case) but their high correlation means that field variations are useful as a measure of the plasma fluctuations. Dukok de Wit and Krasnosel'skikh (1996) recently discussed some of these issues for low latitude solar wind data.

### Calculating $S(m, \tau)$

We note that the calculation of structure functions from a data set does not require the filling of data gaps. Indeed, the data need not even be regularly spaced in time. The algorithms used in the calculation of structure functions in this work allow for such irregularity. We discuss them briefly here: similar algorithms have been used by Horbury *et al.* (1995a, 1996a, b). We first define a set of “bins” spaced in time lag. These need not be of equal width: they are often chosen to be of approximately equal width in log-space. A value of the structure function is calculated for each bin and over a range of powers in the following way. For each point in the data set, absolute differences in the magnetic field are calculated between the point and another point a certain number of measurements later. Therefore, the lag is in terms of data points not time. The time lag between the two points is calculated and the structure function value for the bin in which this time lag lies is altered accordingly: this is done for a range of moments for each difference. Differences are calculated for each point over a range of data lags, and over the entire set of data. This method allows for arbitrarily spaced data points. In practice, data from the Vector Helium Magnetometer (VHM) of the Ulysses magnetic field experiment (Balogh *et al.*, 1992) are taken one or two seconds apart depending on the spacecraft data rate: this rate usually changes twice a day, when small data gaps can occur.

The method outlined above leads to values of the structure function  $S(m, \tau)$  with values of time lag  $\tau$  taken to be the centre of each lag bin, an example of which is shown in Figure 1 for the second order structure function. Values in Figure 1 were calculated from the normal (N) component of 5 days of high resolution magnetic field data taken between 1994 days 130 and 135, when Ulysses was at approximately 63°S and 3.1 AU from the Sun, in the high speed stream from the Sun's Southern polar coronal hole. The normal direction is perpendicular to the Sun-spacecraft line and the cross product of this with the Sun's rotation vector.

We note first that the  $S$ - $\tau$  curve is approximately straight for  $\tau > 10$ s and consequently there is a power law dependence of  $S(m=2)$  on  $\tau$  over this range. We will see later that more accurate analysis reveals variation within this range.

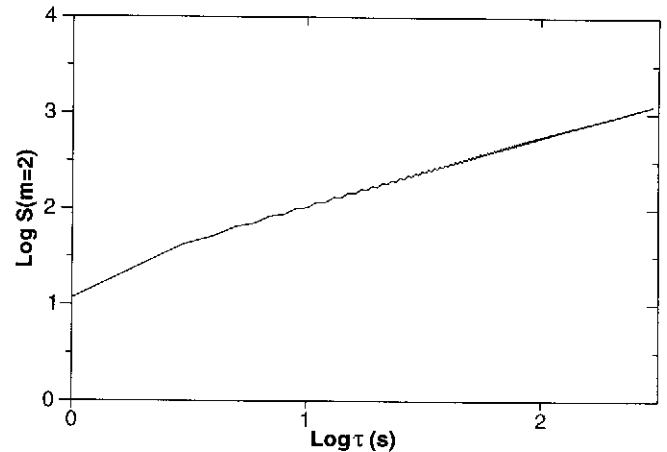


**Figure 1.** Values of the second order structure function  $S(m=2, \tau)$  as a function of time lag  $\tau$ . Results shown are from 5 days of high resolution magnetic field data (N component) taken between 1994 days 130 and 135. Note the approximately linear dependence of  $S$  on  $\tau$  for  $\tau > 10$ s on this log-log plot and the “wiggling” of alternate values as discussed in the text.

Secondly, it is apparent that the curve in Figure 1 “wiggles” slightly – that is, alternate values are higher and lower than the average. This is a result of changes in the spacecraft data rate, and consequently magnetic field sampling rate. At the high data rate, a vector is returned from the sensor once a second; at the low rate, once every two seconds. Therefore, an interval with data rate changes (all intervals considered in this work contain rate changes) will contain sub-intervals with vectors every 1 or 2 seconds. Structure function values with time lags of an odd number of seconds can only result from high rate data, while even lags contain both high and low rate data. If fluctuations during high data rate sub-intervals are larger or smaller than those in low rate sub-intervals on average, then odd lag structure function values will be higher or lower than even lag values, resulting in the “wiggles” seen in Figure 1. This effect only occurs when lag bins are 1 second wide.

### Calculating $g(m)$

The wiggling curve of  $S(m=2, \tau)$  in Figure 1 presents an obstacle to calculating the scaling functions  $g(m)$ . These are generally calculated from least-squares straight line fits of log-log values of  $S$  against  $\tau$ . The oscillating values of  $S(m, \tau)$  can lead to incorrect estimations of the gradients if a simple fit to an even number of points is made – even if an odd number of points is used, the estimate of the error in the gradient will be too large as a result of the large mean variation from the best fit line. The method we have adopted here is to fit to the odd and even lag points separately, producing two gradient estimates over a given range of time scales, and then to combine the two values to give one estimate of the gradient over the range. This method eliminates the effect of the oscillations. Typically, values of  $g(m)$  calculated without allowing for this effect differ from those calculated using the method described above by around 0.1.

Using this method we can estimate  $g(m)$  over a range of moments and compare the values with the predictions of the various models of turbulence presented in the previous section. However, we must first consider errors associated with our structure function estimates.

### Structure function errors

The calculation of structure functions of varying moments at a given scale is essentially the calculation of moments of the distribution of differences in the time series at that scale. Clearly, there is a limit to the number of moments one can reliably calculate. Higher moments emphasise the “wings” of the distribution: when these wings have too few points, structure function estimates are unreliable. Most previously published calculations of heliospheric structure functions have not dealt explicitly with these problems. Such results generally show consistent variation of  $g(m)$  with  $m$  for higher moments, often with a linear dependence and small error bars. However, we will show that such results can be caused by insufficient data and therefore may not be reliable. We will then suggest a semi-empirical criterion for rejecting unreliable structure function estimates based on distribution functions.

Recently, Dukok de Wit and Krasnosel'skikh (1996) presented structure function measurements of turbulent fluctuations near the Earth's bowshock and qualitatively discussed the limitations of high order structure functions, concluding that moments above around 4 were not reliable. In this work we present a quantitative criterion for structure function reliability, and reach a similar conclusion. The advantage of our technique is that it can be applied in an automated way to a large number of measurements, making the analysis of large data sets, while taking into account structure function limitations, possible.

We first consider a set of values  $\delta_i$ ,  $i=1, \dots, N$ , which in this case are absolute differences on a particular time scale  $\tau$ , so  $\delta_i = |b(t_i+\tau) - b(t_i)|$ . We calculate moments of the distribution of values,  $k_m$ , as

$$k_m = \frac{1}{N} \sum_{i=1}^N \delta_i^m \quad (27)$$

We consider the effect of moving one point,  $\delta_j$  to  $\delta'_j$ . Then the moments change to

$$k'_m = \frac{1}{N} \left( (\delta_j')^m + \sum_{i \neq j} \delta_i^m \right) \quad (28)$$

The difference between these values is therefore given by  $(\delta_j'^m - \delta_j^m)/N$ . If  $\delta'_j < \delta_j$  and there are a large number of points near both values, then  $k'_m \sim k_m$ . However, if  $\delta'_j > \delta_j$  and there are few points near  $\delta'_j$  – it is near the tail of the distribution – then for large  $m$ ,  $k'_m \gg k_m$ . In this case, estimates of  $k_m$  are unreliable. Similarly, estimates of  $S(m, \tau)$  are susceptible to this effect. If  $\delta'_j > \delta_j$  then the difference in  $k_m$  is approximately  $\delta_j'^m/N$ . If  $\delta'_j$  is a far outlier, then this value will dominate the calculation of  $k_m$ . We note that values of  $S$  are effectively moments of distributions of differences for a

given time scale. They are, therefore, affected by outliers in this way. Indeed, since these far outliers cause  $S(m)$  to scale as  $\delta_j^m$  for large moments, then when we calculate values of  $g(m)$  by fitting straight lines to the logs of  $S(m)$ , we expect to obtain a linear  $g(m)$  vs.  $m$  relation for sufficiently large moments where  $\delta_j^m$  dominates the sum to calculate  $S(m)$ . This dependence is indeed what is often observed – but it is also expected on the basis of intermittency models. We therefore require a method of distinguishing these cases, to determine whether  $g(m)$  values are the result of accurate measurements of turbulent fluctuations, or the result of insufficiently long data sets.

We note that the occurrence of large differences  $\delta_j$  is a direct consequence of the presence of discontinuities in the magnetic field, although other causes are also likely. In our analysis of fluctuations, we do not wish to eliminate particular types of structure or behaviour, such as discontinuities: we want to remove “unreliable” distributions only. By calculating the distribution functions directly, it is possible to achieve this aim.

Consider a particular jump or step in the magnetic field at a certain point – possibly, but not necessarily, caused by a discontinuity – and its effect on the distribution function of differences on a time scale  $\tau$ . If the change, which we term an “event,” is larger than the average level of fluctuations on this scale, then all differences calculated using data points up to a time  $\tau$  on either side of the change will be affected. If the sampling period of the data is  $t$  then the number of points affected by a single “event” or change will be  $2\tau/t$ . A step in the field can therefore result in  $2\tau/t$  differences which are larger than they should be: this number of points corresponds to a single “event.”

To illustrate these effects, we present some measurements of moments of difference distribution functions in Figure 2. These are calculated from the same data set as used for Figure 1, on a spacecraft time scale of 50 seconds: there are around  $3.1 \times 10^5$  points in this data set. We bin these differences depending on their magnitude: there are 500 bins, each 10pT wide, although only the first 200 are shown: the rest are unpopulated. Figure 2(a) shows the numbers in these bins multiplied by the 1<sup>st</sup> power of the value of the centre of the bin, normalised to the maximum value. The 1<sup>st</sup> moment structure function for  $\tau=50$ s is the sum of the (unnormalised) values in the bins: the difference between calculating directly and calculating using the binned distribution is less than 1%. Panels (b), (c) and (d) show the same calculation for the 2<sup>nd</sup>, 4<sup>th</sup> and 6<sup>th</sup> powers. The distribution for the first moment is generally rather smooth, with a rapidly decaying tail. The value of the corresponding structure function is therefore well defined in the sense that it is not affected by a small number of outlying points.

To quantify and automate the process of rejecting unreliable data, we have used the following method. Firstly, we are only interested in data points which contribute significantly to the total sum. We therefore restrict our attention to those bins which contribute more than 2% of

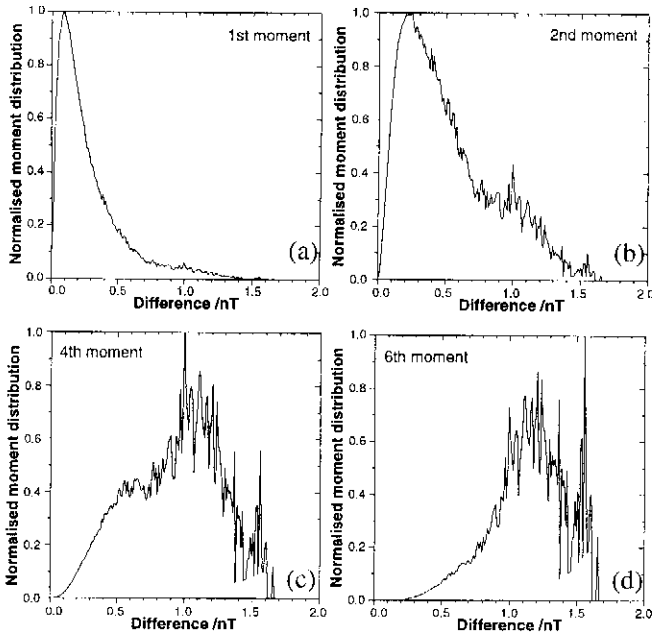


**Figure 2.** Normalised histograms of moment distributions for magnetic field differences on a spacecraft scale of 50s in polar fluctuations. Each panel shows the distribution function of values for a given moment. The structure function of this moment for the 50s scale is the sum over this distribution, although each panel shows values normalised to the maximum value for easy comparison. Moments shown are (a) 1; (b) 2; (c) 4; and (d) 6.

the total sum – that is, which affect the value of  $S$  by 2% or more. If any bin contributes more than 2% to the total (higher numbered bins contribute more to higher moments) then it must contain at least the number of points associated with 10 “events” as defined above. If any point does not meet this criterion, the distribution – and the structure function value calculated from it – is rejected. This procedure is computationally expensive, since the distribution functions must be calculated for each time lag used. It is also somewhat arbitrary, since the fraction of the total sum and the number of events are chosen empirically to reject distributions that appear by eye to be unreliable. However, it has the advantage of being physically motivated and easily implemented.

We can test the effectiveness of the criterion by considering the distributions shown in Figure 2. For the first moment, 2 bins contribute more than 2% of the total – however, they contain well over 10 events (they are at the peak of the distribution): for 1s sampled data and  $\tau=50$ s, one event corresponds to 200 data points. Therefore, this moment is not rejected. For the second moment, it is clear that points in higher bins are weighted more strongly and the peak has moved to a larger value. The tail of the distribution is more ragged as the statistical variation between bins is proportionally larger due to their smaller number of points. A small peak is visible at around 1.6nT. However, no bin contributes 2% or more of the total. This moment is not rejected. Similarly, the fourth moment is kept, although the small peak visible in the second moment distribution is larger. The sixth moment has one point which contributes over 2%, and which has fewer than 10 events.

We can see that this point lies in the 1.6nT peak which is hardly visible in Figure 2(a). The sixth moment is therefore rejected by this criterion. All higher moments are also rejected.

In the example presented here, the first five moments are valid using the error criterion. This is a typical result. We have used this criterion on several 5 day intervals of magnetic field data using time scales from 20 to 300s. These intervals, with over 300,000 data points, usually have the first four moments valid. The fifth moment is sometimes valid, while the sixth is rarely so. The seventh moment has never been valid in the intervals we have studied. While we have used considerably more data points in this study than is common in such work, the rapid decline of the differences distribution functions means that the highest valid moment is probably a rather weak function of the length of the data set and so shorter data sets may have similar numbers of valid moments. We conclude that structure functions of moments above six are unlikely to be reliable in the study of heliospheric turbulence, a result in agreement with Dukok de Wit and Krasnosel’skikh (1996).

The criterion presented here is a simple method of rejecting statistically unreliable data. We emphasise that we do not make any assumptions about the nature of the fluctuations which cause such rejections, but simply reject outliers with too few points. This criterion is used throughout the rest of this paper: we will see that it has a profound effect on the selection of an appropriate model of intermittent turbulence.

There is a drawback of the criterion presented here: at large time lags, the number of data points associated with one event is large and indeed can become a significant fraction of the data set length. If the amplitude of jumps in the field (for example, discontinuities) is larger than characteristic fluctuations on this scale, then the structure function estimate will be significantly influenced by these discontinuities. However, if the fluctuations are generally larger than the jump, then fewer than  $2\tau/t$  points will be affected. This error criterion must therefore be used with care, or modified, for large scales. Here, we use it only for scales of less than 300s, when this effect is not significant.

## 5 Identification of inertial range fluctuations

Horbury *et al.* (1995a) considered the extent of the inertial range in polar flows, and concluded that it extended to around a hundred seconds in the spacecraft frame, although this was a function of solar distance due to the active energy transfer from larger scales. Their identification of the inertial range, in common with most studies, used estimates of the spectral index. Scales where the spectral index was near  $5/3$  or  $3/2$  and relatively invariant with scale were considered to be the inertial range. It is not possible to check for a particular value of the spectral index because intermittency can alter this value. However, Carbone (1994) pointed out that the  $p$  model of intermittency does not affect  $g(3)$  – indeed, we have seen that the models of intermit-



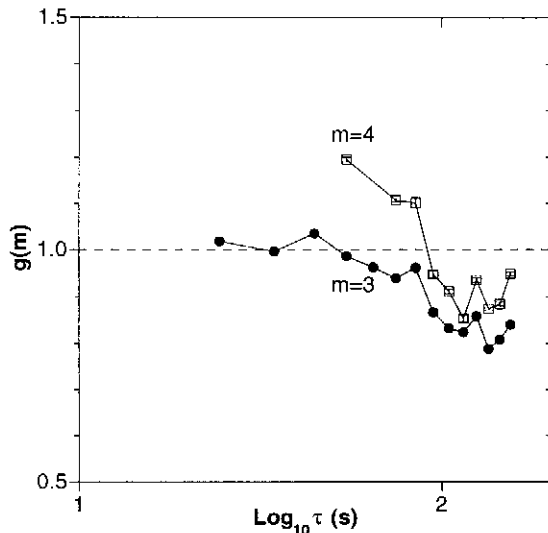


**Figure 3.** Scale dependence of  $g(3)$  and  $g(4)$  for the 5 day interval of magnetic field data used in Figures 1 and 2. Each data point is calculated from a least-squares linear fit to log values of  $g$  against  $\tau$  over a range of 10s. The first range is from 20 to 30s; successive ranges touch but do not overlap.  $g(4)$  is not shown for small time lags: it is statistically unreliable (as discussed in the text) on these scales. Error bars are shown, but are typically smaller than the data symbols and hence not visible.

tency presented here with the K41 energy transfer rate have  $g(3)=1$ . Similarly, those with K-I65 energy transfer have  $g(4)=1$ . Therefore, Carbone (1994) argued that measurements of  $g(3)$  and  $g(4)$  were more reliable indicators of the presence of an inertial range. Such an analysis also introduces the possibility of determining whether the turbulence has a K41 or K-I65 cascade scaling, or some other value. If the energy transfer time is given by Eq.(3) (a K41 cascade) then we would expect to see  $g(3)=1$  as observed for terrestrial turbulence. If the transfer time is given by Eq.(9) (a K-I65 cascade) then we would see  $g(4)=1$ . Carbone (1994) suggested that the data of Burlaga (1991), taken at 8.5 AU, were consistent with a K41 cascade. We note that Burlaga (1991) considered relatively large scales (0.85 hours to 13.6 hours) at 8.5 AU and may therefore have been sampling fluctuations with a rather different character to those on 100s scales in the polar heliosphere.

We proceed to calculate the scale dependence of  $g(3)$  and  $g(4)$  and thereby identify the inertial range of polar fluctuations with greater precision than has previously been possible. We use the same 5 day interval as before, and calculate structure functions for time lags of 20 to 200s. As described in section 4, values of  $g(3)$  and  $g(4)$  are calculated from least-squares linear fits to log-log values of  $S(m=3,\tau)$  and  $S(m=4,\tau)$  against  $\tau$  over ranges of  $\tau$ , with odd and even lags fitted separately and the resulting values – and associated errors – of the gradients combined to produce one value and error for each moment and each time range. The resulting values (and errors, which are generally smaller than the data points) are plotted in Figure 3, showing the scale dependence of both  $g(3)$  and  $g(4)$  in polar flows. More values of  $g(3)$  are shown than of  $g(4)$ : this is because several values of  $g(4)$  were discarded using the error criterion discussed earlier. It is important to realise

that the error estimates in Figure 3 are derived from the linear fits to values of  $S$ . In fact, the large number of time lags used results in a possible oversampling of the data: consequently, variation in  $S$  from one lag to the next is small and error estimates from line fits are also small. True uncertainties in the values of  $g(m)$  may be larger than those shown in Figure 3 but are unlikely to be larger than the trends in  $g(m)$  with changing scale that are visible in the Figure.

From the data in Figure 3, we aim to identify the inertial range. At the largest scales in the Figure, the values of  $g(m)$  are declining with scale: this is indicative of the small scale edge of the transition to  $1/f$  fluctuations at large scales and is consistent with other measurements of the extent of the inertial range (Horbury *et al.*, 1996b; also recent multitapered spectral measurements). The inertial range is, ideally, an extended range of scales where  $g(3)=1$  or  $g(4)=1$ . It is clear from Figure 3 that there is not an extended range of scales where  $g(4)=1$  and therefore not a K-I65 inertial range. In contrast,  $g(3)=1$  is approximately satisfied over a small range of scales, from the smallest shown here (around 20s) to at least 60s and probably to near 100s, where values drop sharply. On this basis, we conclude that the fluctuations on spacecraft time scales under 100s (and hence plasma scales under  $\sim 8 \times 10^7$  km) are consistent with a small inertial range, with a cascade with a K41-like transfer time, in this interval. The significance of this result will be discussed in section 7. We note that the inertial range may extend to smaller scales than 20s, but they cannot be measured reliably using the analysis described here.

We have studied several intervals of magnetic field data at similar solar distances to establish whether the results presented here are representative of fluctuations in this region of the polar heliosphere. We present the results from these intervals in section 7 – however, we note here that they are also consistent with a K41-like cascade.

The identification of  $g(3)=1$ , and hence a K41-like transfer time, constrains the models which can successfully describe the fluctuations. In particular, MHD variations of intermittency models, such as the p model (Carbone, 1993); the  $\beta$  model (Ruzmaikin *et al.*, 1995); or the random  $\beta$  model, which have  $g(4)=1$ , cannot successfully describe the fluctuations in the polar inertial range.

We note that the conjecture of Ruzmaikin *et al.* (1995), that the  $5/3$  spectral index of solar wind turbulence was the result of intermittency altering a fundamentally  $3/2$  Kraichnan-like cascade, is not supported by the results presented here. Ruzmaikin *et al.* (1995) and Horbury *et al.* (1996a) concluded that the Ulysses magnetic field data were consistent with this conjecture. Their conclusions were based on the scaling of structure functions up to moment 10. We suggest that the discrepancy between the earlier results and those presented here is probably due to the statistical unreliability of the high order structure function moments used in the earlier studies.

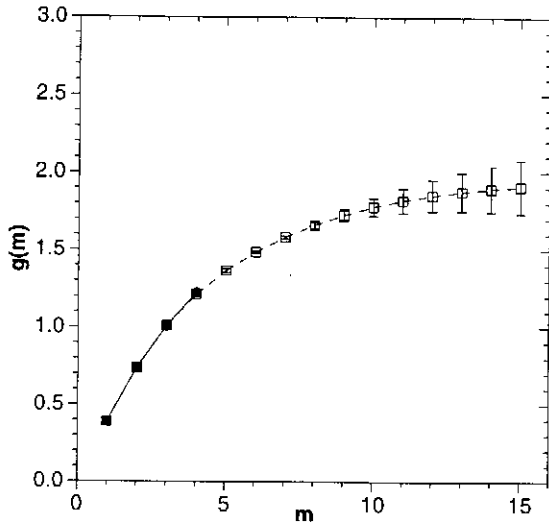


**Figure 4.** Values of the structure function scaling measures  $g(m)$  as a function of moment  $m$ , calculated from least-squares linear fits to log-log values of  $S(m, \tau)$  against  $\tau$  for time scales of 20 to 60s. Open squares are values calculated from all data. Filled circles are values calculated only from data which satisfied the error criterion discussed in the text. Reliable values can only be calculated for moments up to 4.

## 6 Turbulent intermittency

Having established that turbulent fluctuations in polar flows appear to have a K41-like cascade, we proceed to discuss the intermittency of the energy transfer process and determine the model which best describes the data.

Values of  $g(m)$  for moments  $m$  between 1 and 15 are shown in Figure 4. These values were calculated over time scales from 20 to 60s for the same interval as before, 1994 days 130 to 135. These scales are within the inertial range as identified in section 5. Open squares with error bars show values calculated from all structure function values. The squares have the characteristic curved shape of the  $g(m)$  values seen in all heliospheric turbulence studies. We note that  $g(m)$  is approximately linear with  $m$  for high moments.

The filled circles in Figure 4 represent values of  $g(m)$  calculated only from statistically valid values of  $S$  on the basis of the criterion introduced in this work. Values can only be calculated for moments from 1 to 4: above 4, there are no valid values of  $S$  from which  $g$  can be estimated. Therefore, all values of  $g$  for  $m > 4$  are misleading: they are significantly influenced by outlying points. These points appear to be reliable at first sight, following a smooth curve and having small error bars. It is only by considering the distributions explicitly that the reliability of these measurements can be tested.

With only four data points left after unreliable points have been rejected, it appears difficult to distinguish between different intermittent turbulence models. However, we proceed to demonstrate that it is still possible to perform useful tests with these data.

Three of the intermittent turbulence models discussed in this paper (the  $\beta$ , random  $\beta$  and  $p$  models) introduce at least

**Table 1.** Parameters of least-squares best fits to structure function scaling functions for polar fluctuations on spacecraft scales of 20 to 60s, as shown in Figure 4. Deviation values are the root mean squared differences of model fits from the observed data. ‘SL filament’ is the She and Leveque (1994) model with 1D dissipative structures; ‘SL sheet’ is the same model with 2D structures

Model	Parameter name	Value	RMS deviation
$\beta$	$\mu$	0.15	$39 \times 10^{-3}$
Random $\beta$	$x$	0.17	$32 \times 10^{-3}$
SL filament	–	–	$194 \times 10^{-3}$
SL sheet	–	–	$16 \times 10^{-3}$
$p$	$p$	0.79	$7.6 \times 10^{-3}$

one free parameter that can be varied to best fit the data: this parameter is related to the eddy decay process in some way. The random  $\beta$  model of Paladin and Vulpiani (1987) has, in principle, even more parameters but we will use the probability function  $P(\beta) = x \cdot \delta(\beta - 0.5) + (1 - x) \cdot \delta(\beta - 1)$ , which is the same as that used by Paladin and Vulpiani, to reduce the number of parameters to one, the weighting function  $x$ .

The She and Leveque (1994) model does not, in principle, have freely adjustable parameters, although one can alter the characteristic dimension of dissipative structures. Here, we consider variants with K41 energy transfer and filamentary or sheet-like dissipative structures (Eqs. 22 and 25).

We wish to find the model which best describes the available data. For each of the three models with free parameters, we have varied these so as to minimise the least-squares deviation of the values of  $g(m)$  predicted by the model from those observed. We have not used the error estimates on the  $g(m)$  values derived from the line fits to weight these parameter fits because of the problem of oversampling: these error estimates are probably too small. In practice, the best-fit values of parameters are not very different when the error estimates in  $g(m)$  are used.

The non-linear dependence of the model  $g(m)$  functions on  $m$  makes a rigorous confidence test (for example, a  $\chi^2$  test) difficult. Instead, we use the root-mean-square (RMS) deviation of the model values from those observed, which are a byproduct of the fitting process, to establish which class of model is closest to the observations. Values of the least-squares fitted values of the parameters, and the resulting RMS deviations, are presented in Table 1 for the  $\beta$ , random  $\beta$  and  $p$  models. In addition, the RMS deviations from the She and Leveque model with K41 scaling and sheet-like and filament-like dissipative structures are given in Table 1.

The best fit value of  $\mu$  for the  $\beta$  model (Frisch *et al.*, 1978) is rather small, implying that the fluctuations are not very intermittent. Indeed, the value of the weighting function  $x$  for the random  $\beta$  model (Paladin and Vulpiani, 1987) is also rather small, again implying that the fluctuations are largely space-filling. We note, however, that  $x=0.17$  is larger than that found by Paladin and Vulpiani (1987) for terrestrial turbulence, where they found  $x=0.125$ .

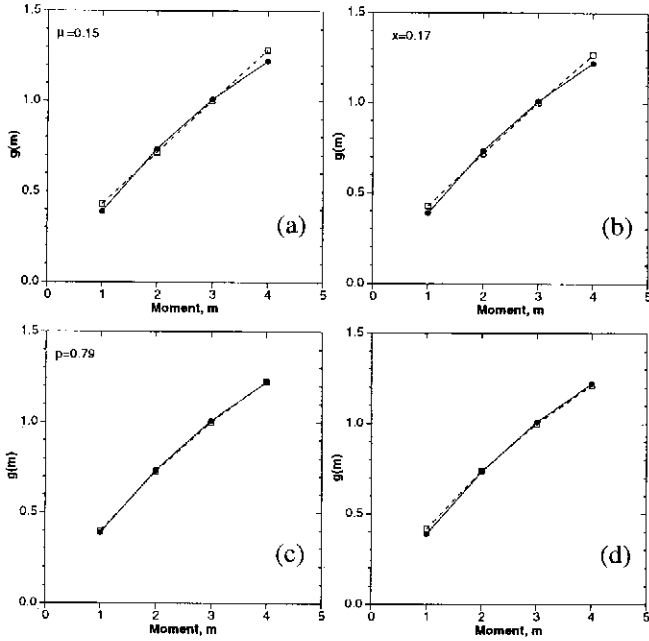


Figure 5. Comparison of observed structure function scaling functions  $g(m)$  of polar turbulence with various turbulence models. Each panel shows observed values as filled circles without error bars: errors are generally similar in size to the circles, but were not used in least-squares fitting models to the data. Panels (a), (b) and (c) show best fit  $g(m)$  values of the  $\beta$  (Frisch *et al.*, 1978), random  $\beta$  (Paladin and Vulpiani, 1987) and  $p$  (Meneveau and Sreenivasan, 1987a, b) models respectively, as open squares along with best-fit values of the relevant parameter. Panel (d) shows  $g(m)$  values of the She and Leveque (1994) model with current sheet dissipation.

The She and Leveque (1994) model, with 1D dissipative structures (“filaments”) is, perhaps unsurprisingly, a poor fit to the data. The 2D variant, with sheet-like dissipative structures, is a considerably better fit than the  $\beta$  and random  $\beta$  models.

It is important to note, however, that the best fits of the  $\beta$ , random  $\beta$  and She and Leveque models are significantly poorer approximations to the observations than that of the  $p$  model (Meneveau and Sreenivasan, 1987a, b). In fact, the RMS deviation for the  $p$  model is less than a quarter that of the  $\beta$  and random  $\beta$  models and less than half that of the She and Leveque model. We conclude that the  $p$  model is the best approximation to the fluctuations on the basis of this data: it has also proved consistently closer to the observations for all other intervals of polar fluctuations that we have analysed.

It is clear that the  $p$  model provides the best approximation to the data when we consider the  $g(m)$  curves for the models. These are shown in Figure 5. Each panel shows the data for 20 to 60s as filled circles. The observed  $g(m)$  values lie on a curve, indicating that intermittency is significant. Panels (a), (b), (c) and (d) show the data compared with the  $\beta$ , random  $\beta$ ,  $p$  and She and Leveque model predictions, respectively. All models have a K41 cascade, and hence  $g(3)=1$ . The  $\beta$  and random  $\beta$  models agree well with the observations, but the  $p$  model fit is considerably better, with deviations being less than the errors on the observations. Visually, the She and Leveque

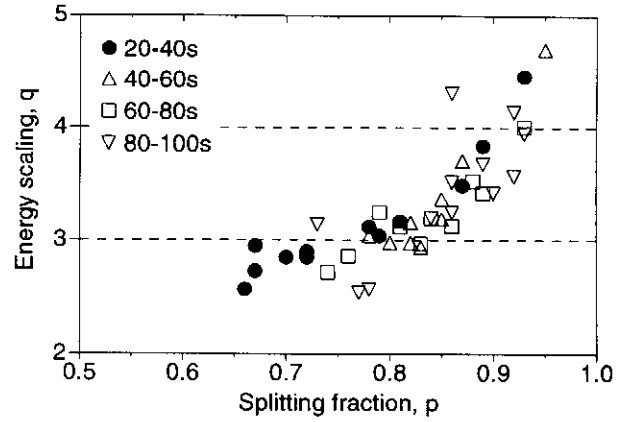


Figure 6. Least-squares fitted values of the intermittency parameter  $p$  and value  $q$  such that  $g(q)=1$ , using the  $p$  model of Meneveau and Sreenivasan (1987b). The data are from 14 intervals, each 5 days in length, containing data taken in high speed ( $>750\text{km/s}$ ) polar flows. Values were calculated over different spacecraft timescales, denoted by different symbols.

model in panel (d) appears almost as good a fit as the  $p$  model: the most obvious difference is in the value of  $g(1)$ . We note that  $g(1)$  is the best defined of all the structure function gradients.

The best fit value of the  $p$  model parameter is 0.79, rather higher than the accepted value for terrestrial turbulence, around 0.7, and higher than that found by Carbone (1994) for the data of Burlaga (1991) which was also around 0.7. The accuracy of this result is not clear from this single measurement, so we have performed a similar analysis on several additional intervals of polar data to produce a distribution of values. This analysis is discussed in the next section.

## 7 Energy transfer

It is possible to perform a fit of the  $g(m)$  data to the  $p$  model and vary not only the intermittency parameter but also the value of  $m$  at which  $g(m)=1$ : we denote this value of  $m$  by  $q$ . That is, one can find the values of  $p$  and  $q$  such that the values

$$g(m) = 1 - \log_2 \left( p^{m/q} + (1-p)^{m/q} \right) \quad (29)$$

are closest to the observed  $g(m)$  values in a least-squares sense. If the range of scales over which the  $g(m)$  values are calculated is an inertial range with a K41 energy transfer rate, then we would expect to find  $q=3$ . Similarly, if the inertial range has a K-165 transfer, we would find  $q=4$ . Such a fit can therefore provide information about both intermittency and energy scaling in the inertial range. We have performed such fits to several intervals of data, the results of which are shown in Figure 6. All the intervals contained data taken in high speed ( $>750\text{km/s}$ ) polar flows, and cover a range of distances and latitudes in both the Northern and Southern polar heliosphere. Values of  $g(m)$  were calculated over four time scales (20-40s; 40-60s; 60-80s; 80-100s) for each interval, and  $p$  and  $q$  estimated as described above. It is clear from Figure 6 that there is a strong  $p$ - $q$  dependence,

with values lying on a curve. The  $p$ - $q$  curve is approximately flat for values of  $p$  from 0.65 to 0.8, near  $q=3$ . There are no values of  $p$  below 0.65. For  $p$  above around 0.8,  $q$  values rise, reaching  $q=4$  for  $p$  around 0.9. However, the curve passes through  $q=4$  and reaches even higher  $q$  values with higher  $p$ . Although the scatter of points is rather large (typically around 0.1 for  $p$  and 0.5 for  $q$ ) the  $p$ - $q$  curve is well defined, leading us to conclude that the  $p$ - $q$  variations are genuinely related, either by a physical mechanism or a systematic analysis effect. This  $p$ - $q$  relation is at first sight surprising, and must be explained if conclusions are to be drawn about “typical” values of both  $p$  and  $q$  in the polar solar wind. In fact, the relation can indeed be explained, in a manner which leads us to conclude that the termination of the curve near the values of ( $p=0.7$ ,  $q=3$ ) is most representative of inertial range polar turbulence.

As we have seen, the inertial range terminates at relatively small scales in the polar solar wind. There is naturally some variation in the extent of the inertial range: in some intervals, it is smaller than others. This can occur because the extent of the inertial range is a function of solar distance in the polar solar wind (Horbury *et al.*, 1996b) but also because of simple variations between different regions: if energy transfer is less steady in one region than another, we would expect a less well-defined inertial range. As a result, for some intervals we expect to find non-inertial behaviour on scales where in other intervals there is an inertial range. Recently, Tu *et al.* (1996) discussed the addition of the  $p$  model of intermittency to a model of evolving turbulence, which is appropriate for fluctuations near the edge of the inertial range, as we would have in the case where the inertial range is smaller than the scale on which fluctuations are measured. In this case, the spectral index is lower, and all structure function values are lower than they would be in the inertial range. Such a reduction can be achieved with the  $p$  model (with inertial range turbulence) by increasing  $p$  and  $q$ , although the precise  $g(m)$  curve is different to the Tu *et al.* (1996) model. When performing a least-squares fit of Eq.(36) to  $g(m)$  values just outside the inertial range, one would therefore expect to see increased  $p$  and  $q$  values compared to inertial range fluctuations. Horbury *et al.* (1997) discussed this issue and showed that within the inertial range, the  $p$  model is a good fit to the observations, but just outside the inertial range fitted values of  $p$  and  $q$  increase and the Tu *et al.* (1996) model is a considerably better fit to the data. This is, of course, unsurprising, but this effect provides an explanation of the data in Figure 6. That is, points with higher  $p$  and  $q$  values reflect fluctuations just *outside* the inertial range: progressively lower values reflect conditions nearer to “ideal” inertial range fluctuations and hence the left hand termination of the  $p$ - $q$  curve reflects the best estimate of  $p$  and  $q$  for polar inertial range turbulent fluctuations. A corollary of this effect is that smaller scale fluctuations should lie nearer the left end of the curve more often than those at larger scales, because smaller scales will generally be more likely to be within the inertial range. It is clear from Figure 6 that

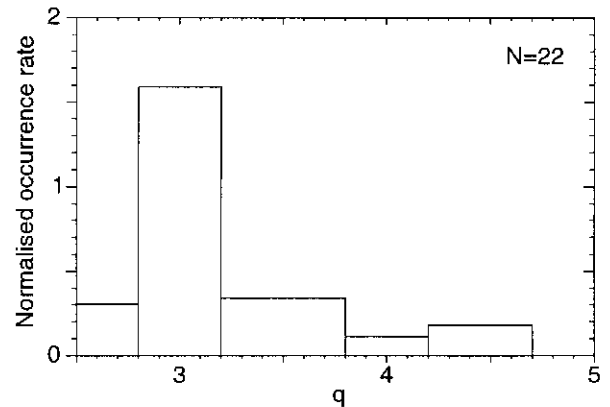


Figure 7. Distribution of least-squares fitted  $q$  values for structure function values on 20-40s and 40-60s scales for polar turbulent fluctuations. K41 corresponds to  $q=3$ ; K-165 corresponds to  $q=4$ . Vertical scale is fraction of total points in each bin, divided by the width of the bin.

this is indeed the case: it is only the smallest scale fluctuations (filled circles) which have the lowest  $p$  and  $q$  values.

We conclude, therefore, that the left hand edge of the curve in Figure 6 most accurately reflects the state of inertial range polar turbulence. Here, to within the effective uncertainty in the values (which is around 0.5 in  $q$  and 0.1 in  $p$ ), we have  $p\sim 0.7$  and  $q\sim 3$ . These values are consistent with a Kolmogorov cascade, with intermittency levels similar to those observed in terrestrial turbulence (e.g. Meneveau and Sreenivasan, 1987a, b) and in at least some other measurements of solar wind turbulence (e.g. Carbone, 1994).

We note that the data in Figure 6 are certainly not consistent with an inertial range K-165 MHD cascade. This is clear from the histogram of values of  $q$  (for only 20-40 and 40-60s scales) presented in Figure 7, which peaks around  $q=3$  but has no peak around  $q=4$ .

## 8 Discussion

In this paper we have attempted to answer two questions regarding the nature of heliospheric turbulence: firstly, which model of intermittent turbulence best describes the observations; and secondly, is the turbulent cascade a Kolmogorov or Kraichnan-Iroshnikov one?

Structure function calculations offer the opportunity of answering both these questions in a rigorous manner. A drawback of using structure functions, however, is the inherent problem of calculating high moments of distributions. We have considered this problem here, and suggested a quantitative criterion for discriminating between “reliable” and “unreliable” structure function values on the basis of the moment distribution. We stress that the criterion is semi-empirical in that an arbitrary numerical criterion is introduced, which is chosen in an *ad hoc* way by considering the observed distributions. This criterion is intended to reject distributions which are influenced by a few far outlying points: it is not intended to identify physically “meaningful” distributions in any way. Intervals which

contain non-stationary data, or non-turbulent data, are – intentionally – not rejected by this criterion. In addition, we stress that this method simply rejects or accepts individual distributions: it does not alter them in any way.

This error criterion appears to be rather successful in rejecting unreliable data in the sense that unusual “kinks” in  $g(m)$  curves, which are due to the influence of far outliers, are eliminated – values of  $g(m)$  above these kinks are rejected. One would expect outliers to produce a linear  $g(m)$  curve at high moments, as does indeed appear to be the case.

After rejecting unreliable data, one is often only left with moments up to 4, 5 or 6. In this paper, we have used rather long intervals of data (5 day intervals of 1 or 2 second resolution, with over  $3 \times 10^5$  points) but moments above 6 are essentially never valid. A consequence of this observation is that one cannot use high order structure functions to describe turbulence properties: while the  $g(m)$  curves at these high moments are smooth and have small apparent errors associated with them, they are not related to the plasma fluctuations – rather, they can be significantly altered by the presence of a few outlying data points. After discarding this unreliable data, we are left with only a few values of  $g(m)$  from which we wish to infer properties of the plasma turbulence. However, this small number of points is sufficient to answer at least one of the two questions we have posed.

To discriminate accurately between intermittency models for inertial range fluctuations, we must first identify the fluctuations’ scaling, or equivalently the scaling of the energy transfer time (see section 2). It is easiest to do this in the inertial range. In principle, in the absence of intermittency it is possible to distinguish K41 and K-I65 scaling from the observed spectral index. However, such measurements are difficult to make in practice and while recent measurements tend to be nearer  $5/3$  than  $3/2$  (e.g. Roberts and Goldstein, 1991), they are not conclusive. The presence of intermittency complicates the problem because it can increase the spectral index, making a precise identification with a particular model more difficult. Indeed, Ruzmaikin *et al.* (1995) suggested that intermittency was the cause of the apparent value of the spectral index near  $5/3$  in polar heliospheric turbulence: they suggested that the underlying spectral index (and hence cascade) in the absence of intermittency was indeed a K-I65 one.

The possibility of using  $g(3)$  and  $g(4)$  to identify K41 or K-I65 turbulence was, to our knowledge, first suggested by Carbone (1994). This method has the considerable advantage of being unaffected by intermittency. Considering the results of Burlaga (1991), using data taken in the far heliosphere at quite large scales, Carbone suggested that the cascade was a Kolmogorov one. On the basis of this method, in section 5 we showed that the inertial range of polar fluctuations, although rather small, appeared to have a K41 scaling. In section 7, using a slightly different method with considerably more data, we obtained the same result. This result is not consistent with the conjecture of Ruz-

maikin *et al.* (1995).

The significant variation of the character of fluctuations in different regions of the polar heliosphere that is clear in Figure 6 means that the identification of Kolmogorov rather than Kraichnan-Iroshnikov turbulence can be no more than tentative. However, the presence of a K41 cascade in solar wind turbulence would not be surprising, for reasons discussed in the next paragraph. It is also no surprise that the cascade does not appear to be a Kraichnan one. Several key assumptions of K-I65, which are vital to the model and distinguish it from K41, such as zero cross helicity and wavevectors parallel to the mean field, are certainly not satisfied in solar wind turbulence. We have discussed the Kraichnan model here because of its continued application to solar wind fluctuations.

We stress that several of the assumptions of the original Kolmogorov and Kraichnan formalisms are violated in the turbulence we have studied. In particular, the inertial range is small; the fluctuations are not homogeneous; and nor are they isotropic. While the inertial range covers around an order of magnitude of scale (see Figure 4 and Horbury *et al.*, 1995a), this is not large compared to the idealised inertial range of theory, covering a wide range of scales. However, behaviour appears to be rather consistent across this range. In fact, the undisturbed, large scale homogeneity of polar flows makes the presence of a well-defined inertial range, despite its small range, more likely than at low latitudes: the gradual decay of large scale fluctuations and input of energy into the inertial range (Horbury *et al.*, 1996b), being unforced, probably proceeds at a rather steady rate. As a result, the inertial range can be maintained even though it only covers a relatively small range of scales.

It is clear that small scale fluctuations are not homogeneous and isotropic in heliospheric turbulence, both at low latitudes (e.g. Matthaeus *et al.*, 1990; Bieber *et al.*, 1996) and in polar flows similar to those studied here (Horbury *et al.*, 1995b): fluctuations tend to be perpendicular to the mean field direction. Indeed, such anisotropy may contribute to the intermittency of the fluctuations as measured here using structure functions. This anisotropy, and in particular the apparent presence of both “slab” and “two-dimensional” fluctuations (e.g. Bieber *et al.*, 1996), may be an important factor in explaining the fact that  $g(3)=1$  in the inertial range. In particular the presence of wavevectors perpendicular to the mean field resulting in Alfvénic fluctuations which do not propagate along the field – and which are therefore not subject to Alfvénic decorrelation – may be important in explaining the apparent K41 cascade. We also note that this result is consistent with some simulation results (e.g. Biskamp and Welter, 1989; Hossain *et al.*, 1995), especially when turbulence is “strong” – the background field is small, while the fluctuations are large. This is, of course, the case for polar fluctuations, at least qualitatively compared to low latitude fluctuations. We do not discuss this result further here, but concentrate on the primary result of this paper, regarding

intermittency models.

We have considered four intermittency models here: the  $\beta$  model (Frisch *et al.*, 1978), its extension as the random  $\beta$  model (Paladin and Vulpiani (1987), the  $p$  model (Meneveau and Sreenivasan, 1987a, b) and the She and Leveque (1994) model. We have not considered the log-normal model (Kolmogorov, 1962), which Burlaga (1991) found to be marginally consistent with observations of hourly-scale velocity fluctuations at 8.5 AU, because this model is not considered to be a physically realistic one (Borgas, 1992).

The models we have considered have all been compared to heliospheric turbulence observations (Burlaga, 1991; Carbone, 1994; Grauer *et al.*, 1994; Ruzmaikin *et al.*, 1995; Horbury *et al.*, 1996a) and there is a clear need to identify the most accurate. All the intermittency models we have described can be used with a K41 or K-I65 cascade – we have used K41 for the reasons described above. The  $p$  model (Meneveau and Sreenivasan, 1987b) describes the observed  $g(m)$  scaling considerably better than the  $\beta$  and random  $\beta$  models, and slightly better than the She and Leveque model with 2D dissipative structures.

The She and Leveque model, while having no freely adjustable parameters, agrees well with the observed scalings. Given that this model, with 1D dissipative structures, agrees well with neutral fluid turbulence measurements, the agreement of the 2D variant with data presented here is remarkable. The physically accessible difference between these two variants is what one would expect given the differences between neutral fluid and MHD flows: the anisotropy produced by the presence of a magnetic field in a magnetofluid results in two dimensional, sheet-like fluctuations. This model certainly merits attention and further analysis, but the  $p$  model best describes the data presented here. Hydrodynamic turbulence is also well described by this model (Meneveau and Sreenivasan, 1987a, b; Borgas, 1992), highlighting the remarkable universality of turbulent intermittency. We have concentrated on the  $p$  model in section 7 because its altered form in Eq.(29) makes it possible to consider variations in both energy transfer and intermittency.

The  $p$  model introduces an empirical parameter which is used to fit the observations. Physically, this parameter describes the uneven energy transfer from parent to daughter eddies. Terrestrial (Meneveau and Sreenivasan, 1987b) and earlier heliospheric observations (Carbone, 1994) found this parameter to be around 0.7. We have found a range of values, but as described in section 7, a value around 0.7 is likely to be representative of inertial range polar fluctuations. We note that Tu *et al.* (1996), while usually finding  $p=0.7-0.8$ , recently found some intervals of Helios data taken near the interplanetary current sheet where  $p>0.8$ , and we hope that future studies will help to further quantify intermittency and its variability and hence lead to a greater understanding of the physical processes involved.

Finally, we stress that the results presented here concern heliospheric turbulence in only one region of the heliosphere. This study will be extended to other data sets taken

at other heliolatitudes and distances to establish whether these results are indeed general: it is not inconceivable that the turbulent cascade may be K-I65-like, for example, in other regions. The remarkable agreement of the  $p$  model with observations offers the hope of providing a simple analytic description of fluctuations for the use in, for example, cosmic ray scattering models as well as a greater understanding of the processes which govern hydromagnetic turbulence throughout the heliosphere and indeed the universe.

*Acknowledgements.* T. S. Horbury is grateful to S. Oughton for useful discussions regarding some aspects of this work. We are grateful to both referees for their constructive and helpful comments. Support for the magnetic field investigation on Ulysses at Imperial College is provided by the U.K. Particle Physics and Astronomy Research Council. T. S. Horbury is supported by a P.P.A.R.C. fellowship.

## References

- Anselmet, F., Gagne, Y., Hopfinger, E. J., and Antonia, R. A., High-order structure functions in turbulent shear flows, *J. Fluid Mech.*, **140**, 63-89, 1984
- Balogh, A., Beek, T. J., Forsyth, R. J., Hedgecock, P. C., Marquedant, R. J., Smith, E. J., Southwood, D. J., and Tsurutani, B. T., The magnetic field investigation on the Ulysses mission: instrumentation and preliminary scientific results, *Astron. Astrophys. Suppl. Ser.*, **92**, 221-236, 1992
- Balogh, A., Smith, E. J., Tsurutani, B. T., Southwood, D. J., Forsyth, R. J., and Horbury, T. S., The heliospheric magnetic field over the South polar region of the Sun, *Science*, **268**, 1007-1010, 1995
- Batchelor, G. K., The theory of homogeneous turbulence, Cambridge University Press, Cambridge, 1953
- Bavassano, B., Dobrowolny, M., Mariani, F., and Ness, N. F., Radial evolution of power spectra of interplanetary Alfvénic turbulence, *J. Geophys. Res.*, **87**, 3617-3622, 1982
- Belcher, J. W. and Davis, L., Large-amplitude Alfvén waves in the interplanetary medium, *J. Geophys. Res.*, **76**, 3534-3563, 1971
- Bieber, J. W., Wanner, W., and Matthaeus, W. H., Dominant 2-dimensional solar-wind turbulence with implications for cosmic-ray transport, *J. Geophys. Res.*, **101**, 2511-2522, 1996
- Biskamp, D. and Welter, H., Dynamics of decaying two-dimensional magnetohydrodynamic turbulence, *Phys. Fluids B*, **1**, 1964-1979, 1989
- Borgas, M. S., A comparison of intermittency models in turbulence, *Phys. Fluids A*, **4**, 2055-2061, 1992
- Burlaga, L. F., Intermittent turbulence in the solar wind, *J. Geophys. Res.*, **96**, 5847-5851, 1991
- Carbone, V., Cascade model for intermittency in fully developed magnetohydrodynamic turbulence, *Phys. Rev. Lett.*, **71**, 1546-1548, 1993
- Carbone, V., Scaling exponents of the velocity structure functions in the interplanetary medium, *Ann. Geophys.*, **12**, 585-590, 1994
- Coleman, P. J., Turbulence, viscosity, and dissipation in the solar-wind plasma, *Astrophys. J.*, **153**, 371-388, 1968
- Dobrowolny, M., Mangeney, A., and Veltri, P., Fully-developed anisotropic hydromagnetic turbulence in interplanetary space, *Phys. Rev. Lett.*, **45**, 144, 1980
- Dukok de Wit, T. and Krasnosel'skikh, V. V., Non-Gaussian statistics in space plasma turbulence: fractal properties and pitfalls, *Nonlinear Processes in Geophysics*, **3**, 262-273, 1996
- Feynman, J. and Ruzmaikin, A., Distributions of the interplanetary magnetic field revisited, *J. Geophys. Res.*, **99**, 17645-17651, 1994
- Feynman, J., Ruzmaikin, A. A., and Smith, E. J., Radial evolution of the high/low frequency breakpoint in magnetic field spectra, in *Proc. of Solar Wind 8*, ed. D. Winterhalter, J. Gosling, S. Habbal, W. Kurth and M. Neugebauer, AIP, 554-557, 1996

- Frisch, U., Turbulence, Cambridge University Press, Cambridge, 1995
- Frisch, U., Sulem, P.-L., and Nelkin, M., A simple dynamical model of intermittent fully developed turbulence, *J. Fluid Mech.*, *87*, 719-736, 1978
- Goldstein, B. E., Smith, E. J., Balogh, A., Horbury, T. S., Goldstein, M. L., and Roberts, D. A., Properties of magnetohydrodynamic turbulence in the solar wind as observed by Ulysses at high heliographic latitudes, *Geophys. Res. Lett.*, *22*, 3393-3396, 1995.
- Grauer, R., Krug, J., and Marliani, C., Scaling of high-order structure functions in magnetohydrodynamic turbulence, *Phys. Lett. A*, *195*, 335-338, 1994
- Horbury, T. S., Balogh, A., Forsyth, R. J., and Smith, E. J., Observations of evolving turbulence in the polar solar wind, *Geophys. Res. Lett.*, *22*, 3401-3404, 1995a
- Horbury, T. S., Balogh, A., Forsyth, R. J., and Smith, E. J., Anisotropy of inertial range turbulence in the polar heliosphere, *Geophys. Res. Lett.*, *22*, 3405-3408, 1995b
- Horbury, T. S., Balogh, A., Forsyth, R. J., and Smith, E. J., Magnetic field signatures of unevolved turbulence in solar polar flows, *J. Geophys. Res.*, *101*, 405-413, 1996a
- Horbury, T. S., Balogh, A., Forsyth, R. J., and Smith, E. J., The rate of turbulent evolution over the Sun's poles, *Astron. Astrophys.*, *316*, 333-341, 1996b
- Horbury, T. S., Balogh, A., Forsyth, R. J., and Smith, E. J., Ulysses observations of intermittent heliospheric turbulence, *Adv. Space Res.*, *19*, 847-850, 1997
- Hossain, M., Gray, P. C., Pontius, D. H., Matthaeus, W. H., and Oughton, S., Phenomenology for the decay of energy-containing eddies in homogeneous MHD turbulence, *Phys. Fluids*, *7*, 2886-2904, 1995
- Iroshnikov, P. S., Turbulence of a conducting fluid in a strong magnetic field, *Sov. Astron.*, *7*, 566-571, 1964
- Kolmogorov, A., The local structure of turbulence in incompressible viscous fluid for very large Reynolds' numbers, *Comptes rendus (Doklady) de l'Academie des sciences de l'URSS*, *30*, 301-305, 1941a
- Kolmogorov, A., Dissipation of energy in the locally isotropic turbulence, *Comptes rendus (Doklady) de l'Academie des sciences de l'URSS*, *30*, 16-18, 1941b
- Kolmogorov, A. N., A refinement of previous hypotheses concerning the local structure of turbulence in a viscous incompressible fluid at high Reynolds number, *J. Fluid Mech.*, *13*, 82-85, 1962
- Kraichnan, R. H., Inertial-range spectrum of hydromagnetic turbulence, *Phys. Fluids*, *8*, 1385-1387, 1965
- Mangeney, A., Grappin, R., and Velli, M., MHD turbulence in the solar wind, in *Advances in solar system magnetohydrodynamics*, eds. E. R. Priest and A. W. Hood, Cambridge University Press, Cambridge, 1991
- Marsch, E. and Liu, S., Structure functions and intermittency of velocity fluctuations in the solar wind, *Ann. Geophys.*, *11*, 227-238, 1993
- Marsch, E. and Tu, C.-Y., Non-Gaussian probability distributions of solar wind fluctuations, *Ann. Geophys.*, *12*, 1127-1138, 1994
- Marsch, E. and Tu, C.-Y., Intermittency, non-Gaussian statistics and fractal scaling of MHD fluctuations in the solar wind, *Nonlinear Proc. in Geophysics*, *4*, 101-124, 1997
- Matthaeus, W. H. and Zhou, Y., Extended inertial range phenomenology of magnetohydrodynamic turbulence, *Phys. Fluids B*, *1*, 1929-1931, 1989
- Matthaeus, W. H., Goldstein, M. L., and Roberts, D. A., Evidence for the presence of quasi-two-dimensional nearly incompressible fluctuations in the solar wind, *J. Geophys. Res.*, *91*, 20673-20683, 1990
- Meneveau, C. and Sreenivasan, S. R., The multifractal spectrum of the dissipation field in turbulence flows, *Nucl. Phys. B (Proc. Suppl.)*, *2*, 1987a
- Meneveau, C. and Sreenivasan, S. R., Simple multifractal cascade model for fully developed turbulence, *Phys. Rev. Lett.*, *59*, 1987b
- Monin, A. S. and Yaglom, A. M., *Statistical Fluid Mechanics: Mechanics of Turbulence*, volume 2, edited by J. L. Lumley, M.I.T. Press, Cambridge, Mass., 1975
- Paladin, G. and Vulpiani, A., Anomalous scaling in multifractal objects, *Phys. Reports*, *156*, 147-225, 1987
- Phillips, J. L., Bame, S. J., Feldman, W. C., Goldstein, B. E., Gosling, J. T., Hammond, C. M., McComas, D. J., Neugebauer, M., Scime, E. E., and Suess, S. T., Ulysses solar wind plasma observations at high Southernly latitudes, *Science*, *268*, 1030-1033, 1995
- Richardson, L. F., *Weather prediction by numerical process*, Cambridge University Press, Cambridge, 1922
- Roberts, D. A. and Goldstein, M. L., Turbulence and waves in the solar wind, *Rev. Geophys., Suppl.*, *932*, 1991
- Roberts, D. A., Klein, L. W., Goldstein, M. L., and Matthaeus, W. H., The nature and evolution of magnetohydrodynamic fluctuations in the solar wind: Voyager observations, *J. Geophys. Res.*, *92*, 11021-11040, 1987
- Ruzmaikin, A. A., Feynman, J., Goldstein, B. E., Smith, E. J., and Balogh, A., Intermittent turbulence in solar wind from the south polar hole, *J. Geophys. Res.*, *100*, 3395-3403, 1995
- She, Z.-S. and Leveque, E., Universal scaling laws in fully developed turbulence, *Phys. Rev. Lett.*, *72*, 336-339, 1994
- Tu, C.-Y. and Marsch, E., MHD structures, waves and turbulence in the solar wind: observations and theories, *Space Sci. Rev.*, *73*, 1-210, 1995
- Tu, C.-Y., Marsch, E., and Rosenbauer, H., An extended structure-function model and its application to the analysis of solar wind intermittency properties, *Ann. Geophys.*, *14*, 270-285, 1996
- Vainshtein, S. I. and Sreenivasan, K. R., Kolmogorov's  $4/5^{\text{th}}$  law and intermittency in turbulence, *Phys. Rev. Lett.*, *73*, 3085-3088, 1994
- Zhou, Y. and Matthaeus, W. H., models of inertial range spectra of interplanetary magnetohydrodynamic turbulence, *J. Geophys. Res.*, *95*, 14881-14892, 1990